Flavin Adenine Dinucleotide Depletion Caused by *electron transfer flavoprotein subunit alpha* Haploinsufficiency Leads to Hepatic Steatosis and Injury in Zebrafish

Ki-Hoon Park,[1] Monika Gooz,[2] Zhi-Wei Ye,[3] Jie Zhang,[3] Gyda C. Beeson,[2] Don C. Rockey,[4] and Seok-Hyung Kim[1]

The electron transfer flavoprotein (ETF) complex, made up of the ETF alpha subunit (ETFA), ETF beta subunit (ETFB), and ETF dehydrogenase (ETFDH), regulates fatty acid β-oxidation activity while scavenging leaked electrons through flavin adenine dinucleotide (FAD)/reduced form FAD ($FADH_2$) redox reactions in mitochondria. Here, we hypothesized that ETF dysfunction-mediated FAD deficiency may result in increased mitochondrial oxidative stress and steatosis and subsequent liver injury. We report that *etfa* haploinsufficiency caused hyperlipidemia, hypercholesterolemia, and hepatic steatosis and injury in adult zebrafish. Further, $etfa^{+/-}$ mutant livers had reduced levels of FAD and glutathione and an increase in reactive oxygen species. Because FAD depletion might be critical in the pathogenesis of the liver lesion identified in $etfa^{+/-}$ mutants, we used riboflavin to elevate FAD levels in the liver and found that riboflavin supplementation significantly suppressed hepatic steatosis and injury in $etfa^{+/-}$ mutants through suppression of oxidative stress and *de novo* lipogenesis in the liver. Additionally, we found that adenosine triphosphate-linked mitochondrial oxygen consumption and mitochondrial membrane potential were reduced in $etfa^{+/-}$ primary hepatocytes and that riboflavin supplementation corrected these defects. *Conclusion:* FAD depletion caused by *etfa* haploinsufficiency plays a key role in hepatic steatosis and oxidative stress-mediated hepatic injury in adult zebrafish. This raises the possibility that people with *ETFA* haploinsufficiency have a high risk for developing liver disease. (*Hepatology Communications* 2021;5:976-991).

Mitochondria are the main cellular source of reactive oxygen species (ROS), which are produced as a by-product of mitochondrial oxidative phosphorylation through the mitochondrial respiratory chain. Mitochondrial respiratory chain disorders are recessive genetic disorders, and homozygous mutations may produce neonatal acute liver failure, hepatic steatohepatitis, or cirrhosis.[1] Although individuals with haploinsufficiency of mitochondrial respiratory chain genes may appear normal, they in fact may be susceptible to developing chronic liver disease, particularly at advanced ages. However, evidence pointing to a link between mitochondrial respiratory chain gene haploinsufficiency and liver disease is lacking to date.

Among the components of the mitochondrial respiratory chain in mammals, the electron transfer flavoprotein (ETF) complex is responsible for transferring

Corrections added on March 8, 2021, after first online publication: in the title, "electron transfer flavoprotein subunit alfa" has been corrected as "electron transfer flavoprotein subunit alpha"

Abbreviations: a1at, alpha-1 antitrypsin; acads/m/l/vl, acyl-coenzyme A dehydrogenase short/medium/long/very long chain; acsl1a, long chain fatty acid-coenzyme A ligase 1a; ALT, alanine aminotransferase; casp3a, caspase 3a; cDNA, complementary DNA; CoA, coenzyme A; col1a1a, collagen, type I, alpha 1; cpt1a, carnitine palmitoyl transferase 1A; dffa, DNA fragmentation factor subunit alpha; dgat2, diacylglycerol O-acyltransferase 2; drp1, dynamin-related protein 1; ETF, electron transfer flavoprotein; Etfa/b, electron transfer flavoprotein alpha/beta subunit; etfdh, electron transfer flavoprotein dehydrogenase; Ex, excitation; FAD, flavin adenine dinucleotide; $FADH_2$, flavin adenine dinucleotide reduced form; fasn, fatty acid synthase; flad1, flavin adenine dinucleotide synthetase; gpx, glutathione peroxidase; GR, glutathione reductase; GSH, glutathione; gsr, glutathione disulfide reductase; gss, glutathione synthetase; GSSG, glutathione disulfide; H&E, hematoxylin and eosin; il1b, interleukin 1b; MADD, multiple acyl-coenzyme A dehydrogenase deficiency; MDA, malondialdehyde; mfn1, mitofusin 1; mmp9, matrix metalloproteinase 9; mRNA, messenger RNA; mtDNA, mitochondrial DNA; mTORC1, mammalian target of rapamycin complex 1; mt-UPR, mitochondrial unfolded protein response; NADH, nicotinamide adenine dinucleotide; NADPH, nicotinamide adenine dinucleotide phosphate, reduced form; nd1, nicotinamide adenine dinucleotide ubiquinone oxidoreductase chain 1; nfkb, nuclear factor kappa-light-chain enhancer of activated B cells; nox, reduced nicotinamide adenine

electrons from at least nine mitochondrial flavoprotein dehydrogenases, including chain length-specific fatty acid acyl-coenzyme A (acyl-CoA) dehydrogenases, to ETF dehydrogenase and then to the respiratory chain.[2-5] Additionally, the ETF complex regulates activities of fatty acid acyl-CoA dehydrogenases during fatty acid β-oxidation, which provides acetyl-CoA to the tricarboxylic acid (TCA) cycle. Subsequently, the TCA cycle provides nicotinamide adenine dinucleotide (NADH) and succinate to mitochondria complex I and II, respectively, for energy production. Mutations in the ETF complex cause multiple acyl-CoA dehydrogenase deficiency (MADD). Although most patients with MADD die at an early age due to multiorgan injury, patients with heterogeneous hypomorphic mutations tend to show liver abnormalities, including hepatomegaly, fatty liver, and hepatic injury, which can occur at juvenile or adult ages.[6-10] Therefore, reduced ETF function caused by haploinsufficiency of a gene in the ETF complex may cause liver disease.

In this study, we have hypothesized that because ETF accepts electrons in the redox process that converts flavin adenine dinucleotide, reduced form ($FADH_2$) to FAD during fatty acid β-oxidation,[11-13] reduced ETF complex activity may cause a decrease in mitochondrial FAD levels and an increase in electron leakage during mitochondrial β-oxidation activity. Further, because mitochondrial FAD functions as an essential cofactor for numerous mitochondrial flavoproteins involved in energy metabolism (such as mitochondrial acyl-CoA dehydrogenases) and redox homeostasis (such as glutathione [GSH] reductase [GR] and thioredoxin (TXN) reductase),[14,15] ETF dysfunction-mediated FAD reduction will result in steatosis and oxidative injury through decreased β-oxidation activity and increased mitochondrial oxidative stress, respectively, in the liver.

In this paper, we determined liver abnormalities caused by *etf alpha subunit* (*etfa*) haploinsufficiency in adult zebrafish and examined if supplementation with

dinucleotide phosphate oxidase; OCR, oxygen consumption rate; opa1, optic atrophy type 1; ORO, Oil Red O; polg, DNA polymerase gamma, catalytic subunit; qRT-PCR, real-time quantitative polymerase chain reaction; ribo, riboflavin; ROS, reactive oxygen species; sod, superoxide dismutase; srebp, sterol regulatory element binding protein; TBA, thiobarbituric acid; TC, total cholesterol; TG, triglyceride; TMRM, tetramethylrhodamine methyl ester; tnfa, tumor necrosis factor alpha; txn, thioredoxin; txnl, thioredoxin-like; wt, wild type.

Received August 20, 2020; accepted January 18, 2021.

Additional Supporting Information may be found at onlinelibrary.wiley.com/doi/10.1002/hep4.1691/suppinfo.

Supported in part by Cell and Molecular Imaging Shared Resource, Medical University of South Carolina (MUSC) Cancer Center (Support Grant P30 CA138313 to M.G.), South Carolina Center of Biomedical Research Excellence (SC COBRE) in Oxidants, Redox Balance, and Stress Signaling (P20 GM103542 to K.P., M.G., Z.Y., J.Z., G.B., and S.K.), SC COBRE in Digestive and Liver Diseases (P20 GM130457 to M.G.), MUSC Digestive Disease Core Center (P30 DK123704 to D.C.R. and S.K.), and MUSC Shared Instrumentation (Grant S10 OD028663 to M.G.).

View this article online at wileyonlinelibrary.com.

DOI 10.1002/hep4.1691

Potential conflict of interest: Nothing to report.

ARTICLE INFORMATION:

From the [1]Department of Medicine; [2]Department of Drug Discovery and Biomedical Sciences; [3]Department of Cell and Molecular Pharmacology and Experimental Therapeutics; [4]Digestive Disease Research Center, Medical University of South Carolina, Charleston, SC, USA.

ADDRESS CORRESPONDENCE AND REPRINT REQUESTS TO:

Seok-Hyung Kim, Ph.D.
Department of Medicine, Medical University of South Carolina
Drug Discovery Building
70 President Street
Charleston, SC 29425
E-mail: kims@musc.edu
Tel.: +1-843-876-2338

riboflavin (a precursor of FAD) would reverse liver abnormality in *etfa* heterozygous mutants.

Materials and Methods

ZEBRAFISH HUSBANDRY AND RIBOFLAVIN TREATMENT

Care of zebrafish was in accordance with guidelines and regulations of the National Institutes of Health Guide for the Care and Use of Laboratory Animals and Medical University of South Carolina (MUSC) Division of Laboratory Animal Resources. All experiments on zebrafish were approved by the Institutional Animal Care and Use Committee of MUSC (protocol #3364). Zebrafish strains used in this study included *etfa*$^{+/+}$ (wild-type siblings) and *etfa*$^{+/vu463}$ heterozygous mutants[16] in the AB/Tuebingen (TU) (wild-type) background. We used 20-month-old wild-type and *etfa*$^{+/-}$ male and female siblings for experiments in (Figs. 1 and 2). For all experiments in Figs. 3-7, we used 10-month-old male fish (Figs. 3-7). Groups of wild-type and *etfa*$^{+/-}$ siblings were maintained in separated 2-gallon glass tanks with or without riboflavin treatment (0.6 mg/L). We fed zebrafish tetramin flakes, as described,[17] twice per day (10 mg/fish/meal). Fresh water with or without riboflavin was exchanged every other day.

BLOOD COLLECTION AND BIOCHEMICAL ANALYSIS

Blood collection was performed by inserting a glass capillary needle into the zebrafish's dorsal aorta, as reported.[18] Zebrafish blood was obtained by using a heparinized needle for blood collection along the body axis and posterior to the anus in the region of the dorsal aorta. Blood was collected from zebrafish after a 20-hour fasting period. Blood glucose level was measured with Bayer Contour NEXT Diabetes EZ meter (Bayer AG, Germany) using Contour NEXT Blood Glucose Test Strips. Blood samples were diluted 1:10 in phosphate-buffered saline. After centrifugation, the supernatant containing serum was collected. Triglyceride (TG), total cholesterol (TC), and alanine aminotransferase (ALT) levels in diluted serum were measured with kits according to the manufacturer's protocol (Thermo Scientific #TR22421 for TG; Wako #439-17501 for TC; Pointe Scientific #A7526 for ALT).

HISTOLOGY

Hematoxylin and eosin (H&E) staining was performed in paraffin sections of livers by the Pathology Core Facility at MUSC. For Oil Red O (ORO) staining on transversely sectioned larvae, frozen sections (10 μm) were dried at room temperature for 5 minutes. Then, 150 μL of ORO solution (5% ORO in 60% isopropyl alcohol) was applied to slides for 30 seconds, washed with distilled water, and mounted using 75% glycerol.

QUANTITATIVE REAL-TIME POLYMERASE CHAIN REACTION

RNA was isolated from adult zebrafish liver using Trizol as per the manufacturer's instructions (Invitrogen #15596-026), and complementary DNA (cDNA) was reverse transcribed using a SuperScript III First-Strand kit (Invitrogen #18080-051). Total RNA was extracted from three livers each from wild-type and *etfa*$^{+/-}$ siblings, and then equivalent amounts of RNA was pooled for cDNA synthesis. Real-time quantitative polymerase chain reaction (qRT-PCR) was performed with a thermal cycler (CFX96 Real-Time System; Bio-Rad Laboratories) with 45 cycles, using 50 ng cDNA, 200 pmole/μL gene-specific primers (Supporting Table S1), and SsoAdvanced Universal SYBR Green Supermix (Bio-Rad Laboratories #172-5274). *Glyceraldehyde 3-phosphate dehydrogenase* (*gapdh*) was used as reference, and relative quantification was calculated using the double-delta C_t ($\Delta\Delta C_t$) method. qRT-PCR was run in at least triplicate for each assay.

INTRACELLULAR ROS

Intracellular ROS was measured by using the OxiSelect *In Vitro* ROS/reactive nitrogen species (RNS) Kit from Cell Biolabs (San Diego, CA), as per the manufacturer's protocol. Lysates were collected (1 mg/mL) and immediately subjected to the ROS/RNS measurement. The fluorescent intensity of fluorophore dichlorofluorescein, which was formed by peroxide oxidation of the nonfluorescent precursor dichlorodihydrofluorescin (DCFH), was detected at 480 excitation (Ex)/530 emission (Em) (BMG LABTECH CLARIOstar, Germany). DCFH with lysis buffer was used as a blank control.

GSH AND GLUTATHIONE DISULFIDE LEVELS

Quantitative determinations of GSH and GSH/glutathione disulfide (GSSG) levels in liver lysates were performed using the enzymatic-recycling method, as described.[19] Proteins in the extracts from wild-type and *etfa*$^{+/-}$ adult livers were precipitated by sulfosalicylic acid, and the supernatant was then divided into two tubes. For reduced GSH, the supernatant was incubated with the thiol fluorescent probe IV, and fluorescent intensities were measured at 400 Ex/465 Em. For total GSH (GSH+GSSG), the supernatant was neutralized by triethanolamine and incubated with the reduction system (containing nicotinamide adenine dinucleotide phosphate, reduced form [NADPH] and GR) at 37°C for 20 minutes. GSSG was calculated based on the results from reduced GSH and total GSH.

MALONDIALDEHYDE MEASUREMENT

Liver lysates were analyzed by the thiobarbituric acid (TBA) reactive substances assay to evaluate changes in levels of oxidized species, using malondialdehyde (MDA) as a standard. MDA level was measured with the lipid peroxidation assay kit (BioVision, #K739-100). Briefly, deproteinized liver lysates by perchloric acid and then MDA in the sample are reacted with TBA to generate the MDA-TBA adduct, which can be detected at 532 nm.

GR ACTIVITY

The GR activity assay was based on the reduction of GSSG to GSH in the presence of NADPH. GSH then reacts with 5,5′-dithiobis-(2-nitrobenzoic acid) (DTNB) to generate 5-thio-(2-nitrobenzoic acid) (TNB), which is associated with an increase in the absorbance at 412 nm; the rate of this increase is directly proportional to the GR activity in the sample. The extinction coefficient (ε) for TNB is 14.15 mM^{-1} cm^{-1}. Briefly, the assay was performed with 1 mM GSSG (Sigma), 0.05 mM NADPH (Sigma), 1.5 mM DTNB, and zebrafish lysate (after using the Bio-Rad Bio-Spin 6 to remove endogenous GSH) or with GR (Sigma) as a positive control in 0.1 M potassium phosphate buffer with 1 mM ethylene diamine tetraacetic acid, pH 7.5 (final volume, 200 μL). Absorbance was read at 412 nm with the CLARIOstar Plus microplate reader (BMG LABTECH).

ANALYSIS OF RELATIVE MITOCHONDRIAL DNA COPY NUMBER

Genomic DNAs from wild-type and *etfa*$^{+/-}$ mutant livers with or without riboflavin treatment (n = 6 per each group) were isolated and diluted in water. For qRT-PCR analysis, we used 25 ng cDNA. Samples were run in triplicate and mitochondrial DNA (mtDNA) content was calculated by the $2^{-\Delta\Delta Ct}$ method whereby all *NADH ubiquinone oxidoreductase chain 1* (*nd1*; the mtDNA target) C_t values were normalized to *eukaryotic translation elongation factor 1 alpha* (*ef1a*; a nuclear DNA target), as described.[20]

ZEBRAFISH PRIMARY HEPATOCYTE CULTURE

Primary cell cultures of hepatocytes were obtained from adult zebrafish, as described.[21] Six zebrafish from each wild-type and heterozygous *etfa* livers were used.

SEAHORSE XF MITOCHONDRIA STRESS ANALYSIS

Zebrafish primary hepatocytes were plated onto an Agilent Seahorse XF96^e plate (FluxPak #102416-100) at 2 × 10^5 cells/well. The Seahorse XF96^e Analyzer (Agilent, Santa Clara, CA) was used to measure the basal levels of the oxygen consumption rate (OCR) and extracellular acidification rate (ECAR) as well as the OCR and ECAR of cells in the presence of electron transport chain inhibitors and uncouplers (oligomycin, 1 μM; carbonyl cyanide-p-trifluoromethoxyphenylhydrazone (FCCP), 1 μM; rotenone, 2 μM; antimycin A, 2 μM), using the standard software algorithm.

The day before analysis, the sensor cartridge was placed in the calibration buffer provided by the Agilent Seahorse analyzer. The following day, the media was replaced by low-phosphate Dulbecco's modified Eagle's medium buffer and warmed in a 28°C non-CO_2 incubator. The injection ports of the sensor plate were filled with 25 μL of compounds or vehicle diluted in buffer, and the sensor plate was placed into the XF-96e instrument for calibration. During the calibration of the sensor, the plate was placed into the Sartorius "Zoom" microscope and was imaged and analyzed for percentage of cell confluency. After calibration, the calibration fluid plate was removed, and the cell plate was loaded for analysis. The measurement protocol

was 2 minutes mix and 3 minutes measurement. There were four rate measurements after each injection (basal levels, oligomycin, FCCP, and antimycin/rotenone), and each injection had three measurement cycles. OCR was finally normalized to percentage confluency/well. Statistics and graphs were generated using Agilent Seahorse Wave Desktop software.

IMAGING OF MITOCHONDRIAL MEMBRANE POTENTIAL

Cells plated in eight-well chamber slides (MatTek) were loaded with 200 nM tetramethylrhodamine methyl ester (TMRM; Millipore Sigma #T5428) in complete growth media. Slides were imaged using a Cytation 5 Cell Imaging Multi-Mode Reader (BioTek Instruments, Inc., Winooski, VT) with a 20× Plan Fluorite Objective, numerical aperture 0.45. TMRM fluorescence was quantified using the red fluorescent protein imaging cube, which contained a 523-nm light-emitting diode and a 531/40-nm Ex filter, 593/40-nm Em filter, and 568-nm dichroic mirror. A seven-slice *z*-stack was collected during experiments. A single-image projection was then created from the *z*-stack using the focus stacking algorithm within the Gen5 software. TMRM fluorescence intensities of mitochondria were calculated and expressed as arbitrary fluorescence units.

STATISTICAL ANALYSIS

Statistical significance was determined by the two-tailed Student *t* test, using GraphPad Prism 8 software (GraphPad Software, Inc.), and $P < 0.05$ was considered significant. Quantitative data were expressed as mean ± SD.

Results

etfa HAPLOINSUFFICIENCY INDUCES HEPATIC STEATOSIS AND INJURY WITH INCREASED MESSENGER RNA EXPRESSION OF GENES ASSOCIATED WITH INFLAMMATION, FIBROSIS, AND LIPOGENESIS

In previous work, we demonstrated that the homozygous *etfa* null mutation resulted in severe and progressive liver injury, characterized by hepatomegaly, steatosis, and an inflammatory lesion from 5 days post-fertilization (dpf) to 8 dpf.[16] Although heterozygous *etfa* mutants appear to develop and grow normally, we hypothesized that reduced ETF function caused by *etfa* haploinsufficiency causes liver injury in adult zebrafish.

To test our hypothesis, we initially studied the morphology of $etfa^{+/-}$ zebrafish livers. In the normal liver, cords of hepatocytes were readily identified. In contrast, an increased number of injured hepatocytes in a disorganized pattern were visualized in $etfa^{+/-}$ zebrafish livers; these hepatocytes had an accumulation of eosinophilic material in the hepatocyte cytoplasm with a reduction in normal cytosol staining (Fig. 1A, top panel, marked with red arrow heads). ORO staining indicated a significant increase in the amount of lipid drops in $etfa^{+/-}$ livers (Fig. 1A, bottom panel).

In addition, we found that *etfa* haploinsufficiency induced a significant increase in serum ALT activity in both male and female zebrafish (Fig. 1B). We also found that there was a striking increase in expression of messenger RNAs (mRNAs) associated with *de novo* lipogenesis (*sterol regulatory element binding protein* (*srebp*)*1*, *srebp2*, and *fatty acid synthase* [*fasn*]) in $etfa^{+/-}$ livers (Fig. 1C). Further, we found increased mRNA expression in genes associated with inflammation (*tumor necrosis factor alpha* [*tnfa*], *nuclear factor kappa-light-chain enhancer of activated B cells* [*nfkb*], *interleukin 1b* [*il1b*], and *matrix metalloproteinase 9* [*mmp9*]), cell death (*caspase 3a* [*casp3a*] and *alpha-1 antitrypsin* [*a1at*]), and fibrosis (*collagen, type I, alpha 1* [*col1a1a*]) in $etfa^{+/-}$ livers (Fig. 1G). In aggregate, these data demonstrate that *etfa* haploinsufficiency results in hepatic steatosis and injury, possibly due to increased expression of genes associated with lipogenesis and inflammation in adult zebrafish. Although *col1a1a* mRNA expression in the liver was increased, significant fibrosis labeling in liver sections could not be identified using picrosirius red staining (data not shown).

Notably, *etfa* haploinsufficiency reduced mRNA expression of *etfa* as expected. We also found that mRNA expression of other components in the ETF complex (*etfb* and *etf dehydrogenase* [*etfdh*]) were decreased in the liver the same as *etfa* (Fig. 1D), which suggests that *etfa* haploinsufficiency may also regulate activity of the ETF complex at the transcriptional level. Transcriptional reduction of *etfa* by gene haploinsufficiency caused a significant decrease in expression of Etfa at the protein level, which was determined by immunofluorescence staining and western blot using anti-Etfa antibody in liver lysates (Fig. 1E,F).

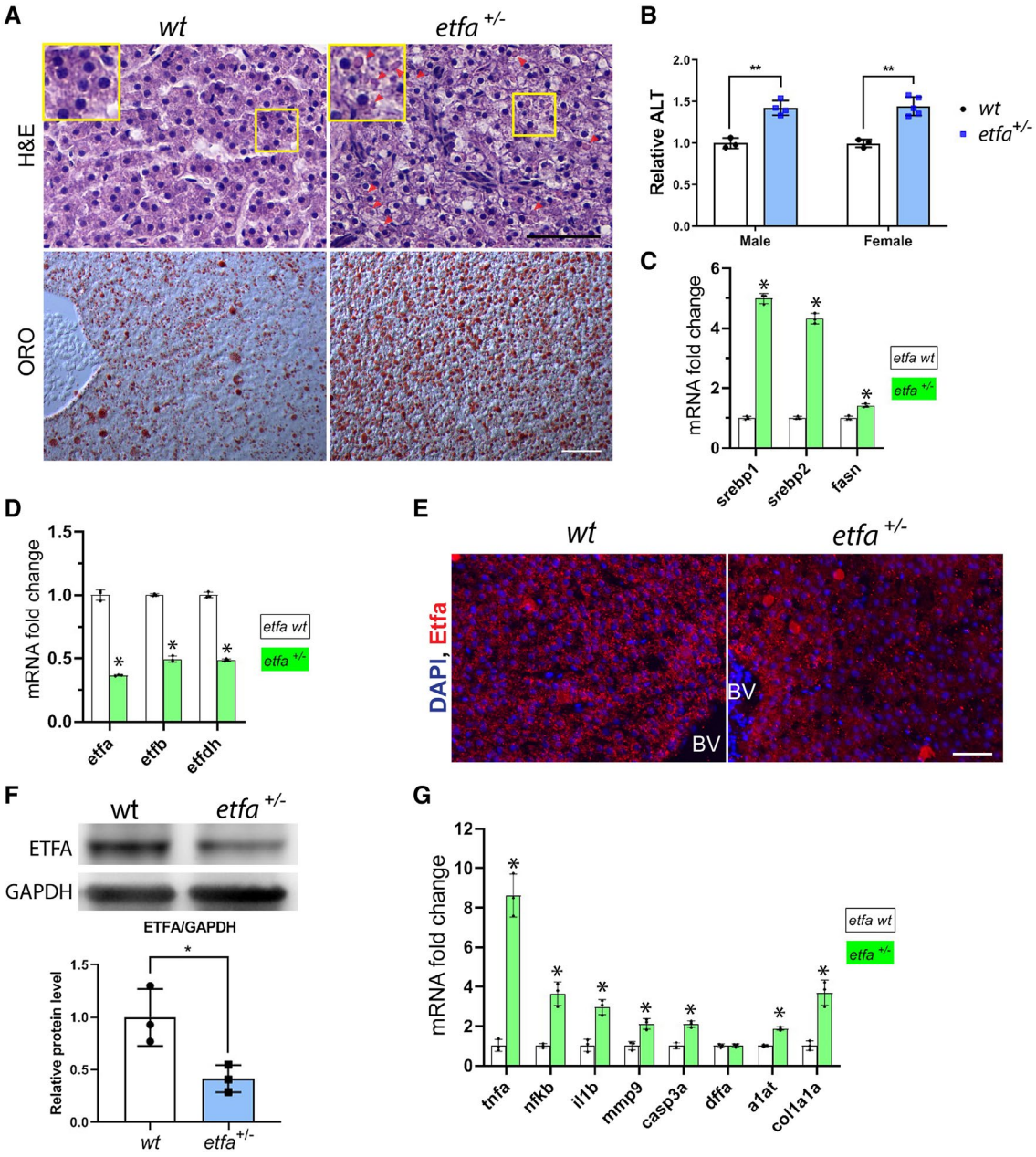

FIG. 1. *Etfa* haploinsufficiency induces hepatic injury and steatosis in adult zebrafish. (A) Representative images show hepatocyte ballooning and accumulation of cytosolic components (note eosinophilic cytoplasmic droplets marked with arrow heads) in hepatocytes in *etfa*$^{+/-}$ livers (H&E staining). Magnified views (yellow rectangles) are shown. In the bottom panels, sections were stained with ORO (representative images are shown, n = 5/5); scale bar, 50 μm. (B) Relative serum ALT levels in *etfa*$^{+/-}$ siblings compared to the wild type (n = 3 to 5). (C) Livers were harvested, and pooled total RNA was subjected to qRT-PCR (see Materials and Methods) to determine relative mRNA expression genes associated with *de novo* lipogenesis (*srebp1*, *srebp2,* and *fasn*). (D) Relative mRNA expression of genes of *etfa*, *etfb,* and *etfdh* (*P < 0.05 vs. the wild type). (E) Immunofluorescence staining with anti-Etfa antibody (red) on wild-type and *etfa*$^{+/-}$ liver sections; scale bar, 50 μm. Nuclei were stained with DAPI. (F) Relative amount of Etfa protein in wild-type and etfa$^{+/-}$ liver lysates (n = 3). (G) Relative mRNA expression of genes associated with inflammation (*tnfa, nfkb, il1b,* and *mmp9*), cell death (*casp3a* and *dffa*), injury (*a1at*), and fibrosis (*col1a1a*). Pooled RNAs (from three livers per group) were used for qRT-PCR analysis. *P < 0.05, **P < 0.005 vs. the wild type. Data in bar graphs represent mean ± SD. Abbreviations: BV, blood vessel; DAPI, 4′,6-diamidino-2-phenylindole; GAPDH, glyceraldehyde 3-phosphate dehydrogenase.

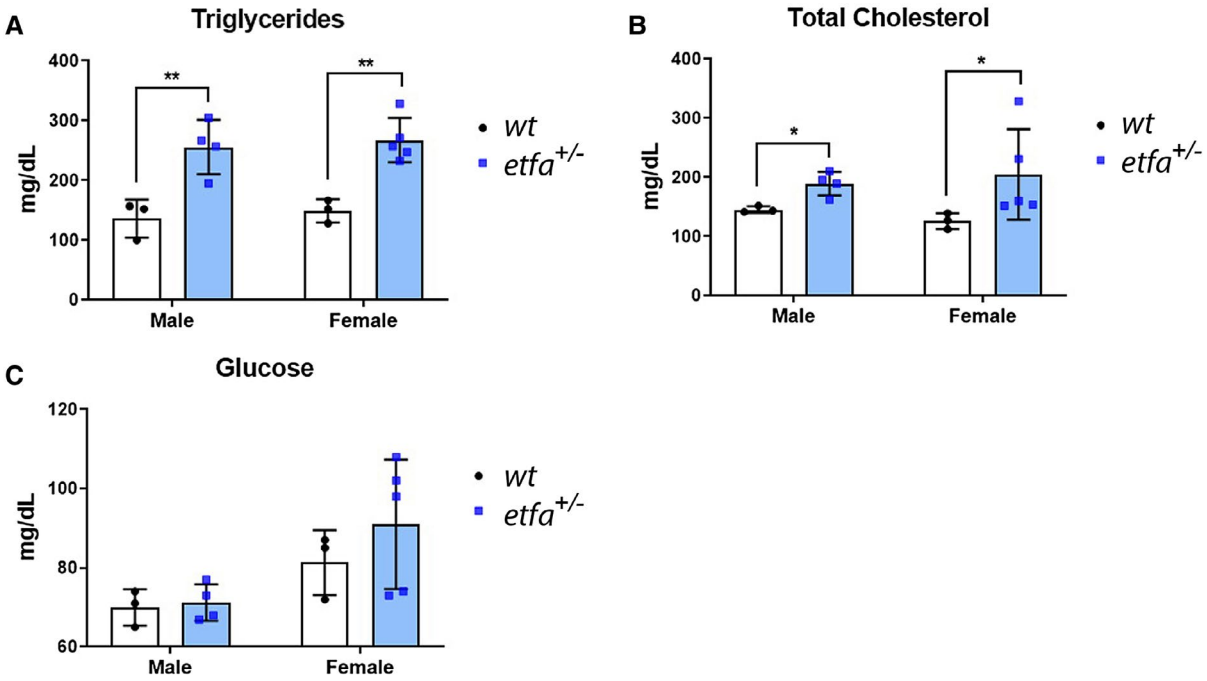

FIG. 2. *Etfa*$^{+/-}$ zebrafish exhibit hyperlipidemia and hypercholesterolemia. (A) Blood was drawn (see Materials and Methods), and serum TGs, (B) TC, and (C) glucose were measured in male and female wild-type (n = 3, white bars) and *etfa*$^{+/-}$ siblings (n = 4, blue bars). $^{*}P < 0.05$, $^{**}P < 0.005$ versus the wild type. Data represent mean ± SD.

etfa HAPLOINSUFFICIENCY CAUSES AN INCREASE IN SERUM TG AND CHOLESTEROL LEVELS

The *etfa*$^{+/-}$ male and *etfa*$^{+/-}$ female zebrafish have 1.7-fold and 1.8-fold higher serum TG levels, respectively, than wild-type siblings (Fig. 2A). TC analysis was similar, with 1.3-fold and 1.8-fold higher cholesterol levels in *etfa*$^{+/-}$ males and females, respectively, than wild-type siblings (Fig. 2B). Of note, there did not appear to be significant changes in serum glucose levels (Fig. 2C). These data indicate that *etfa* haploinsufficiency induced a hypertriglyceridemia and hypercholesterolemia phenotype in adult zebrafish and raise the possibility that there is reduced fatty acid β-oxidation in *etfa*$^{+/-}$ mutants.

etfa HAPLOINSUFFICIENCY INCREASES OXIDATIVE STRESS IN THE LIVER

Given the role of the ETF complex as an electron acceptor during mitochondrial β-oxidation, increased electron leakage may result in increased hepatic superoxide formation and oxidative stress. To investigate oxidative stress in the liver, we measured ROS, GSH, GSSG, and MDA (a standard marker for lipid peroxide) levels in liver lysates from control and *etfa*$^{+/-}$ mutants (Fig. 3A-D). We found a 1.6-fold increase in ROS levels in *etfa*$^{+/-}$ livers. Although there was a significant decrease in GSH (0.6-fold) in *etfa*$^{+/-}$ livers, GSSG levels were not changed. Further, MDA levels in *etfa*$^{+/-}$ livers were increased compared to wild-type livers.

Interestingly, the activity of GSH reductase (Gsr), an enzyme that converts GSSG to GSH, was increased (1.4-fold) in *etfa*$^{+/-}$ mutants (Fig. 3E), perhaps triggered by a compensatory response. Consistent with the possibility was the finding of a significant increase in *glutathione synthetase* (*gss*) and Gsr mRNA expression (Fig. 3F). Additionally, *etfa* haploinsufficiency increased mRNA expression of genes associated with *de novo* GSH synthesis in the liver (Supporting Fig. S1). These data suggest that GSH reduction in *etfa*$^{+/-}$ mutants might result from limited substrates for GSH synthesis.

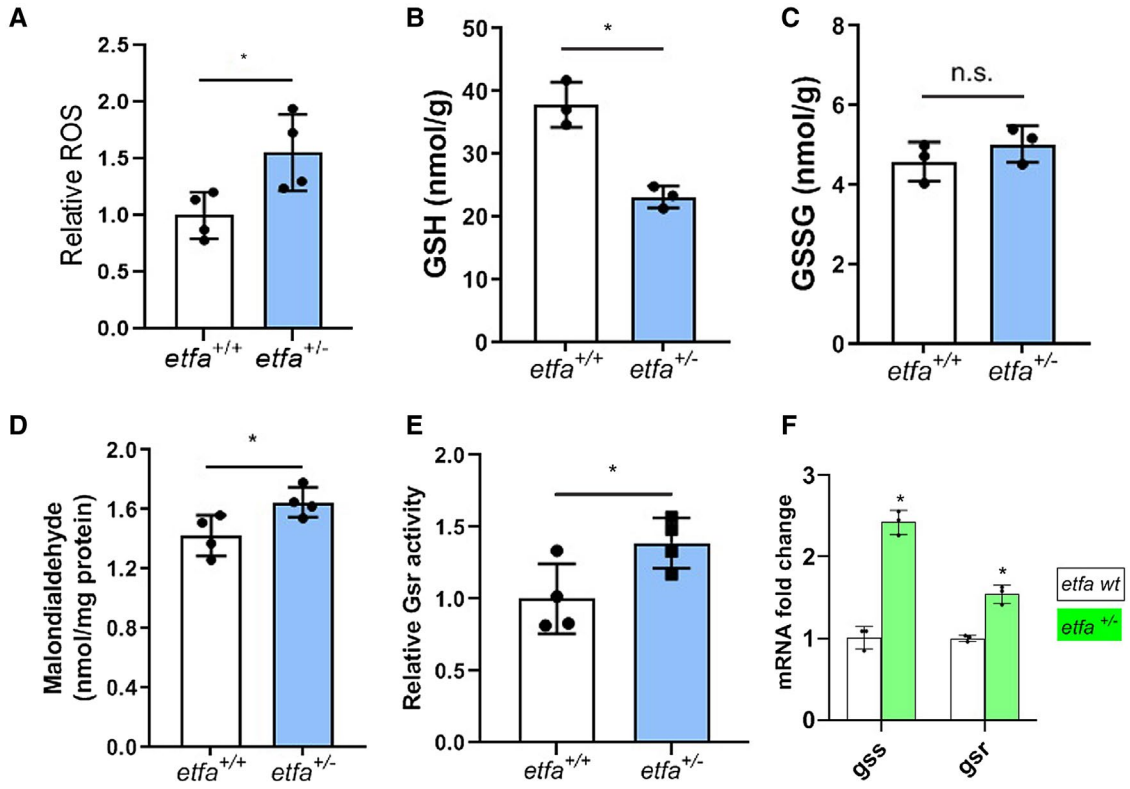

FIG. 3. *Etfa* haploinsufficiency increases oxidative stress in the liver. (A) ROS (H_2O_2), (B) GSH, (C) GSSG, and (D) MDA were measured in wild-type and *etfa*$^{+/-}$ male siblings (see Materials and Methods). (E) Relative activity of Gsr in *etfa*$^{+/-}$ siblings versus the wild type (n = 4), and (F) mRNA expression of *gss* and *gsr*. Error bars show the mean ± SD; *$P < 0.05$. Abbreviation: n.s., not significant.

RIBOFLAVIN SUPPLEMENTATION RESOLVES FAD DEPLETION AND INHIBITS HEPATIC INJURY IN THE *etfa*$^{+/-}$ LIVER

etfa haploinsufficiency reduced *etfa* mRNA expression as well as that of other components of the ETF complex (*etfb* and *etfdh*) (Fig. 1B). Because ETF is important for the redox reaction ($FADH_2$ to FAD conversion process) during mitochondrial fatty acid β-oxidation, reduced ETF activity will lead to FAD reduction. As expected, FAD levels were decreased by 25% in *etfa*$^{+/-}$ livers compared to wild-type siblings (Fig. 4A). To test whether riboflavin, the substrate for FAD synthesis supplementation, can restore reduced FAD in the *etfa*-haploinsufficient state, we exposed wild-type and *etfa*$^{+/-}$ zebrafish to riboflavin containing water for 1 week (0.6 mg/L). This led to significantly increased hepatic FAD levels in both the wild type (1.14-fold) and the *etfa*$^{+/-}$ mutants (1.42-fold) (Fig. 4A). Riboflavin supplementation also led to reduced serum ALT levels in *etfa*$^{+/-}$ adults, almost reducing levels to normal. There was also a slight reduction in ALT levels in the wild-type zebrafish after riboflavin treatment, although they were not statistically significantly different than controls (Fig. 4B). Riboflavin treatment also reduced hepatic injury in *etfa*$^{+/-}$ mutants (Fig. 4B,C); there was a reduced number of abnormal hepatocytes, which appeared in a more normal pattern, with fewer intracytoplasmic eosinophilic inclusions. We found moderate (*tnfa* and *mmp9*) or significant (*nfkb* and *il1b*) decreases in inflammatory marker genes, and a significant reduction (*casp3a* and *DNA fragmentation factor subunit alpha* [*dffa*]) in cell death marker genes. Riboflavin treatment led to normalization of *col1a1a* mRNA in *etfa*$^{+/-}$ livers (Fig. 4D).

Because it is possible that mitochondrial FAD reduction induced by *etfa* haploinsufficiency may cause a compensatory increase in FAD synthesis, we compared mRNA expression of mitochondrial *FAD synthetase* (*flad1*) in wild-type and *etfa*$^{+/-}$ livers with or without riboflavin treatment (for 1 week). Interestingly,

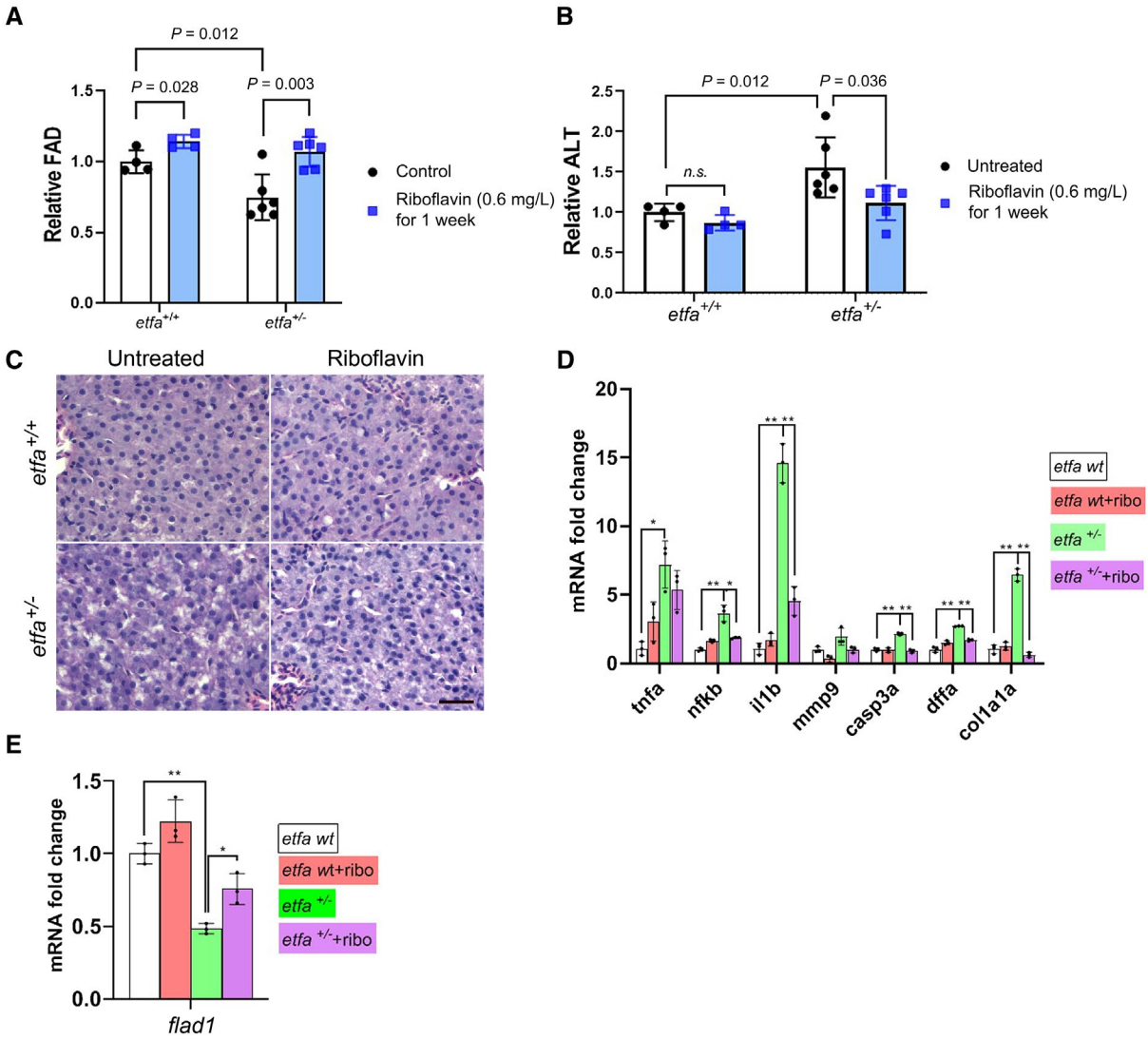

FIG. 4. Riboflavin supplementation suppresses hepatic injury and genes associated with inflammation in *etfa*$^{+/-}$ livers. Adult zebrafish were exposed to riboflavin containing water (0.6 mg/L) for 1 week, with water replacement (with riboflavin) once per day. Whole livers were harvested, and relative amounts of (A) FAD levels and (B) serum ALT levels were measured in *etfa*$^{+/-}$ with (white bars) or without (blue bars) riboflavin treatment compared to the wild type (*etfa*$^{+/+}$) (see Materials and Methods) (n = 4 to 6). (C) Representative images of H&E-stained liver sections in the wild type and *etfa*$^{+/-}$ mutants with or without riboflavin treatment (n > 6 per each); scale bar, 25 μm. (D) Total RNA was isolated from whole livers as above, and mRNA expression of genes associated with inflammation (*tnfa, nfkb, il1b,* and *mmp9*), cell death (*casp3a* and *dffa*), injury (*a1at*), and fibrosis (*col1a1a*) from pooled RNA were measured by qRT-PCR (see Materials and Methods). (E) Changes in relative mRNA expression levels of *flad1* were also measured. An equal amount of total RNA from three livers were pooled and used for cDNA synthesis; the same amount of cDNA was used for qPCR analyses. Error bars show mean ± SD; $^{*}P < 0.05$, $^{**}P < 0.005$. Abbreviation: n.s., not significant.

we found a significant decrease in *flad1* mRNA levels in *etfa*$^{+/-}$ livers, with riboflavin treatment leading to a moderate increase in *flad1* mRNA expression in both wild-type and *etfa*$^{+/-}$ livers (Fig. 4E). This result suggests that FAD reduction was caused by reduced ETF function in a redox reaction (from $FADH_2$ to FAD) as well as reduced FAD synthesis in mitochondria.

RIBOFLAVIN SUPPLEMENTATION SUPPRESSES OXIDATIVE STRESS IN THE *etfa*$^{+/-}$ LIVER

To determine the mechanisms by which riboflavin suppresses hepatic injury and inflammation in *etfa*$^{+/-}$ mutants, we first investigated changes in

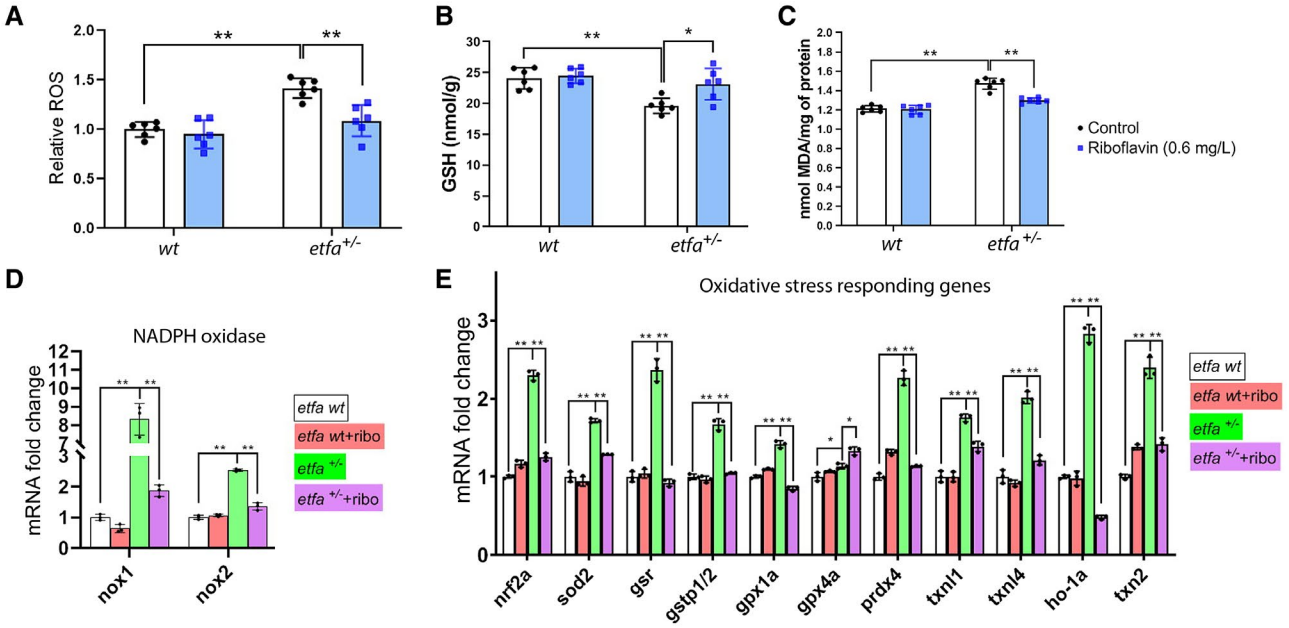

FIG. 5. Riboflavin supplementation suppresses oxidative stress in *etfa*$^{+/-}$ mutant livers. Adult zebrafish were exposed to riboflavin, as in Fig. 4. (A) Relative ROS, (B) GSH levels, and (C) MDA levels in wild-type and *etfa*$^{+/-}$ livers from untreated or riboflavin-treated adult zebrafish were measured (see Materials and Methods) (n = 6 per group). Relative mRNA expression of (D) NADPH oxidases and (E) oxidative stress-responding genes was measured (see Materials and Methods; three livers were used to make normalized RNA; $^{*}P < 0.05$, $^{**}P < 0.005$). Abbreviations: gstp1/2, glutathione S transferase pi 1 and 2; ho-1a, heme oxygenase 1a; nrf2, nuclear factor erythroid 2-related factor 2; prdx4, peroxiredoxin 4.

oxidative stress in the liver. As above, *etfa* haploinsufficiency caused increases in ROS (1.4-fold) and MDA (1.2-fold) and decreases in GSH (0.8-fold) levels. Riboflavin supplementation significantly suppressed elevated ROS and MDA levels while restoring reduced GSH levels in *etfa*$^{+/-}$ livers (Fig. 5A-C). We also determined expression of NADPH oxidases, key enzymes producing superoxides, as over activity in those genes can lead to oxidative stress and cell damage (Fig. 5D). We found significant increases in *NADPH oxidase* (*nox*)*1* and *nox2* expression in *etfa*$^{+/-}$ livers. Riboflavin treatment significantly suppressed elevated expression of *nox1* and *nox2* in *etfa*$^{+/-}$ livers. Thus, *etfa* haploinsufficiency-mediated FAD reduction increased oxidative stress in the liver.

We also examined other constituents associated with the oxidative stress response and the effect of riboflavin on them (Fig. 5E). The expression of *nuclear factor erythroid 2* (*nrf2*), considered a master regulator of anti-oxidative response, was highly elevated in *etfa*$^{+/-}$ livers. An increase of superoxide can induce *superoxide dismutase 2, mitochondrial* (*sod2*) mRNA expression to reduce mitochondrial oxidative stress. Because increased oxidative stress triggers transcriptional activation of genes associated with the oxidative stress response, we analyzed genes in two main systems governing cellular redox reactions: the glutathione system and the thioredoxin system. We found mRNAs of genes associated with both glutathione (*gsr, glutathione S-transferase pi 1* [*gstp1*]*/2,* and *glutathione peroxidase 1a* [*gpx1a*]*/4a*) and thioredoxin (*peroxiredoxin 4* [*prdx4*], *thioredoxin-like 1* [*txnl1*], and *txnl4*) systems were increased by *etfa* haploinsufficiency. Furthermore, we found a significant increase in *txn2*, which encodes for mitochondria-specific thioredoxin. Thus, *etfa* haploinsufficiency elevated expression of oxidative stress-responding genes in the liver, and riboflavin supplementation suppressed expression of those genes close to levels found in wild-type livers. We also found that *gpx4a* (a phospholipid hydroperoxidase that protects cells against membrane lipid peroxidation[22,23]) was moderately increased after riboflavin treatment, which suggests that riboflavin supplementation may protect the liver from lipid peroxides by increasing *gpx4a* expression in *etfa*$^{+/-}$ livers.

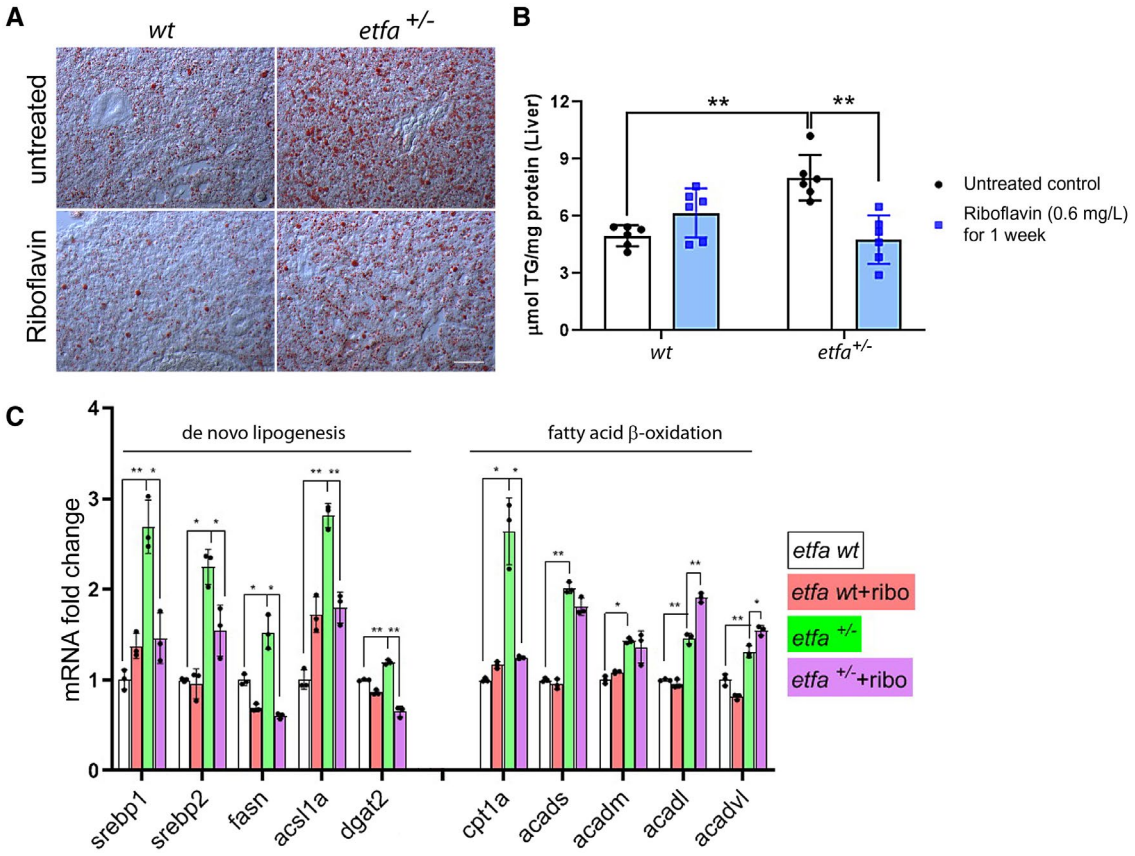

FIG. 6. Riboflavin supplementation attenuates hepatic steatosis in *etfa*$^{+/-}$ livers by suppressing mRNA expression of genes in *de novo* lipogenesis and lipid uptake. Adult zebrafish were exposed to riboflavin, as in Fig. 4. (A) Representative images of ORO staining (n = 5 per group) in the wild type and *etfa*$^{+/-}$ mutants with or without riboflavin treatment for 1 week; Scale bar, 50 µm. (B) TG analysis in liver lysates from wild-type and *etfa*$^{+/-}$ livers with or without riboflavin treatment (n = 6 per group). (C) Relative mRNA expression of genes associated with *de novo* lipogenesis (*srebp1, srebp2, fasn, acsl1a,* and *dgat2*) and fatty acid β-oxidation (*cpt1a, acads, acadm, acadl*, and *acadvl*) was measured by qRT-PCR (see Materials and Methods; n = 3 per group, $^{*}P < 0.05$, $^{**}P < 0.005$).

RIBOFLAVIN SUPPLEMENTATION BLOCKS *De Novo* LIPOGENESIS AND FATTY ACID ACYL-CoA UPTAKE IN THE *etfa*$^{+/-}$ LIVER

Increased hepatic TG levels were reduced to normal levels by riboflavin treatment in *etfa*$^{+/-}$ livers (Fig. 6A). To further investigate the mechanism by which riboflavin resolves steatosis, we investigated genes associated with lipid metabolism (Fig. 6B). We found significant increases in genes associated with *de novo* lipogenesis as well as fatty acid β-oxidation. In *etfa*$^{+/-}$ livers, mRNA expression of *srebp1* and *srebp2*, which are essential for lipid and cholesterol biogenesis, was increased. mRNA levels of key lipogenic enzymes involved in fatty acid *de novo* synthesis were also significantly increased, including *fasn*, which catalyzes the synthesis of palmitic acid from acetyl-CoA and malonyl-CoA; *long chain fatty acid-coenzyme A ligase 1a* (*acsl1a*), a gene essential for the synthesis of long-chain fatty acid acyl-CoA; and *diacylglycerol O-acyltransferase 2* (*dgat2*), a gene essential for the final reaction in TG synthesis. In addition, mRNAs encoding enzymes involved in fatty acid β-oxidation were increased, including *c*arnitine palmitoyl transferase 1A (cpt1a), a key enzyme transporting fatty acyl-CoA into mitochondria, and fatty acid acyl-CoA dehydrogenases (*acyl-CoA dehydrogenase short/medium/long/very long chain* [*acads*], [*acadm*], [*acadl*], and [*acadvl*]) were found in *etfa*$^{+/-}$ livers, which are likely increased

as a compensatory response to resolve reduced mitochondrial β-oxidation activity in *etfa*$^{+/-}$ livers.

Riboflavin supplementation attenuated elevation of mRNAs involved in *de novo* lipogenesis (*srebp1*, *srebp2*, *fasn*, *acsl1a*, and *dgat2*) and mitochondrial fatty acid transport (*cpt1a*) in *etfa*$^{+/-}$ livers (Fig. 6B). The data suggest that increased *de novo* lipogenesis and mitochondrial fatty acid uptake appear to lead steatosis in the *etfa*$^{+/-}$ liver and that riboflavin can rescue this abnormality.

However, riboflavin supplementation did not suppress the elevated mRNA expression of fatty acid acyl-CoA dehydrogenases (*acads*, *acadm*, *acadl*, and *acadvl*). This finding implies that these enzymes need to be highly expressed to compensate reduced fatty

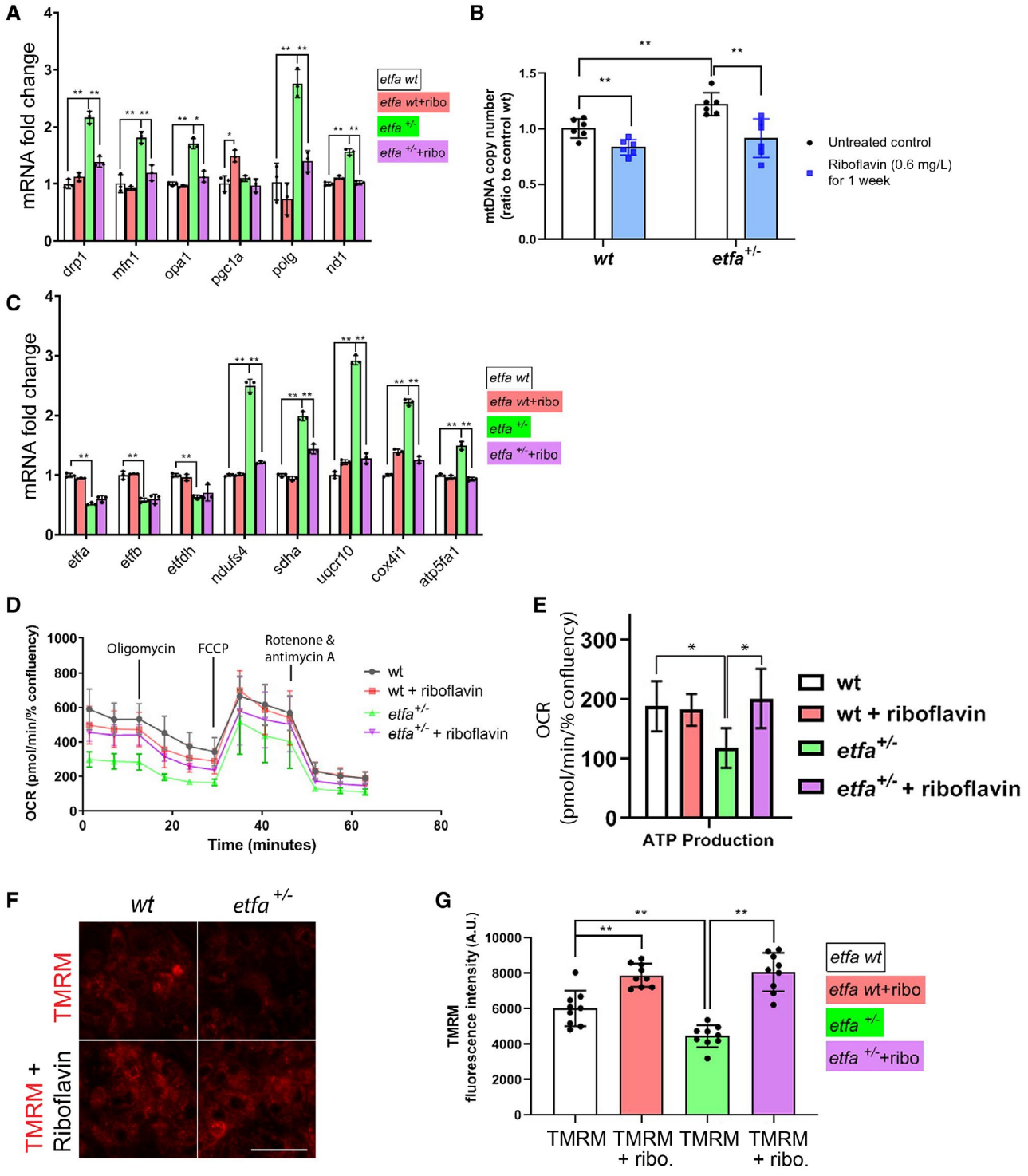

FIG. 7. Effects of riboflavin on mitochondria in *etfa*$^{+/-}$ livers. Adult zebrafish were exposed to riboflavin, as in Fig. 4. Livers were harvested and (A) relative mRNA expression of genes associated with mitochondrial homeostasis and biogenesis, (B) relative copy number of mtDNA, and (C) relative mRNA expressions of genes in the ETF complex and mitochondrial complexes (I to V) in wild-type or *etfa*$^{+/-}$ livers with or without riboflavin treatment were measured by qRT-PCR (see Materials and Methods). (D) Hepatocytes were isolated, incubated for 3 days with or without riboflavin (0.6 mg/L), and OCR analysis was performed using Seahorse XF96 (see Materials and Methods). (E) ATP production-associated OCR in each group (n = 4; $^{*}P < 0.05$, $^{**}P < 0.005$). (F) Representative fluorescence images of TMRM-loaded wild-type and *etfa*$^{+/-}$ hepatocytes with or without riboflavin treatment; scale bar, 50 μm. (G) Mitochondrial membrane potential was compared by TMRM fluorescence intensity of hepatocytes in (F). Abbreviations: ATP, adenosine triphosphate; atp5fa1, adenosine triphosphate synthase F1 subunit alpha; A.U., arbitrary units; cox4i1, cytochrome *c* oxidase subunit 4 isoform 1; min, minutes; ndufs4, nicotinamide adenine dinucleotide:ubiquinone oxidoreductase subunit S4; pgc1a, peroxisome proliferator-activated receptor gamma coactivator 1-alpha; sdha, succinate dehydrogenase complex flavoprotein subunit A; uqcr10, ubiquinol-cytochrome *c* reductase 10.

acid β-oxidation activity in *etfa*$^{+/-}$ livers. Thus, both increased expression of these enzymes and riboflavin supplementation are required to achieve a normal level of β-oxidation in *etfa*$^{+/-}$ livers.

EFFECTS OF *etfa* HAPLOINSUFFICIENCY AND RIBOFLAVIN SUPPLEMENTATION ON MITOCHONDRIAL BIOGENESIS/FUNCTION

We hypothesized that reduced mitochondrial activity could affect mitochondrial biogenesis in the *etfa*$^{+/-}$ liver. Therefore, we analyzed mRNA expression of genes involved in mitochondrial biogenesis and function.[24] We found a significant increase in a number of these mRNAs, including *dynamin-related protein 1* (*drp1*), a gene required for mitochondrial fission; *optic atrophy type 1* (*opa1*), which plays a role in mitochondrial fusion as well as cristae stabilization; *DNA polymerase gamma, catalytic subunit* (*polg*), a mitochondrial DNA polymerase; *nd1*, a subunit of NADH dehydrogenase encoded from the mitochondrial DNA; and *mitofusin 1* (*mfn1*), a gene important for mitochondrial fusion (Fig. 7A). Of note, *peroxisome proliferator-activated receptor gamma, coactivator 1 alpha* (*pgc1a*) mRNA expression, a putative master regulator of mitochondrial biogenesis, was not changed. Riboflavin supplementation attenuated increased expression of *drp1*, *mfn1*, *opa1*, *polg,* and *nd1* in *etfa*$^{+/-}$ livers (Fig. 7A).

Mitochondrial number was determined by comparing the relative copy number of genomic DNAs for *nd1* (a mitochondrial gene) and *ef1a* (a nuclear gene) in wild-type and *etfa*$^{+/-}$ livers. We found a significant increase of mtDNA copy number in *etfa*$^{+/-}$ livers (Fig. 7B) compared to wild-type siblings, and riboflavin supplementation decreased mtDNA copy number in both wild-type and *etfa*$^{+/-}$ livers (Fig. 7B).

We also found that expression of mRNAs encoding for mitochondrial electron transport complex members I to V were significantly elevated in *etfa*$^{+/-}$ livers (Fig. 7C). This could represent a compensatory response to reduced mitochondrial electron transport chain activity. Additionally, this could be a result of an increased number of mitochondria. Importantly, we found that riboflavin supplementation did not affect expression of ETF complex genes (*etfa*, *etfb,* and *etfdh*), while it suppressed increased mRNAs of genes representing components in complex I to V (Fig. 7C). This may be because riboflavin does not suppress elevated mRNA expression in fatty acid acyl-CoA dehydrogenases (Fig. 6C); a decreased ETF complex may interfere with full activity of these enzymes, even after riboflavin treatment.

To examine mitochondrial activity in wild-type and *etfa*$^{+/-}$ hepatocytes with or without riboflavin treatment, we performed a mitochondria stress analysis (using Seahorse XF96) in primary hepatocyte cultures from wild-type and *etfa*$^{+/-}$ livers. We found significant decreases in adenosine triphosphate production-associated OCRs in *etfa*$^{+/-}$ hepatocytes; riboflavin supplementation completely rescued decreased OCRs in *etfa*$^{+/-}$ hepatocytes (Fig. 7D,E). Reduced mitochondrial activity in *etfa*$^{+/-}$ hepatocytes may cause a decrease in mitochondrial membrane potential ($\Delta\Psi$). Therefore, we examined $\Delta\Psi$ in primary hepatocytes from wild-type and *etfa*$^{+/-}$ siblings using the potential indicator dye TMRM. Microscopic image analysis of hepatocytes showed significantly decreased TMRM fluorescence in *etfa*$^{+/-}$ hepatocytes compared to wild-type cells; riboflavin treatment elevated TMRM intensity in both wild-type and *etfa*$^{+/-}$ hepatocytes (Fig. 7F,G).

In aggregate, the data suggest that an increase in the total number of mitochondria in *etfa*$^{+/-}$ mutant livers was caused by a compensatory response to reduced mitochondrial activity caused by *etfa* haploinsufficiency. Oxygen consumption analysis and mitochondrial membrane potential analysis indicated that actual mitochondrial activity might be lower than in the wild type. Riboflavin supplementation diminished the compensatory responses associated with mitochondrial biogenesis and function (Fig. 7A-C) by increasing the activity of mitochondria in *etfa*$^{+/-}$ mutant livers.

Discussion

The ETF complex regulates activities of mitochondrial flavoprotein dehydrogenases that include fatty acid acyl-CoA dehydrogenases. Thus, ETF dysfunction leads to fatty acid accumulation, which may result in development of fatty liver disease. Patients with MADD with biallelic mutations in genes consisting of the ETF complex develop distinct liver abnormalities, including hepatomegaly, fatty liver, and hepatic injury, throughout infant to adult ages.[6-10] Although reduced ETF function by a deleterious mutation in a single allele does not cause severe defects in the liver, a gene haploinsufficiency may increase risk to develop chronic liver disease. This possibility is supported by our finding that heterozygous *etfa* mutant zebrafish with reduced ETF function exhibit hepatic steatosis and injury as a result of FAD depletion, increased lipogenesis, and increased oxidative stress.

Although the significance of riboflavin/FAD deficiency in liver disease has not been studied well, previous studies showed that a riboflavin-deficient diet may induce fatty liver disease in cats,[25] rats,[26] and ducks,[27] possibly due to reduced mitochondrial β-oxidation activity. In addition, chronic alcohol consumption hinders riboflavin absorption in the intestine[28-30] and may result in a reduction in FAD in the liver; it could therefore contribute to hepatic steatosis in alcoholic liver disease. Thus, riboflavin/FAD depletion may be important in the pathogenesis of nonalcoholic and alcoholic chronic liver disease, and riboflavin supplementation may be an effective therapy for both types of diseases.

We noticed less severe hepatic injury in younger *etfa*$^{+/-}$ zebrafish (10 months old; Fig. 4C) compared to older mutants (20 months old; Fig. 1A), which suggests that hepatic injury may progress as *etfa*$^{+/-}$ mutants age. However, further experiments will be required to more rigorously address the impact of age on hepatic injury in zebrafish.

It is unknown whether *etfa* haploinsufficiency can reduce FAD levels in the liver. We showed that *etfa* haploinsufficiency was enough to reduce FAD levels in the liver (Fig. 4A), which might be caused by decreased ETF function in the redox reaction of $FADH_2$ to FAD in *etfa*$^{+/-}$ livers. Additionally, significant increases in mRNA expression of FAD-dependent acyl-CoA enzymes could potentiate FAD reduction in the *etfa*$^{+/-}$ liver and lead to development of liver disease (Fig. 6B).

Reduced FAD levels appear to have a strong impact on folding and maintenance of the native structure in ETF and acyl-CoA dehydrogenases,[31-34] which suggests that ETF haploinsufficiency-induced FAD reduction may induce the mitochondrial unfolded protein response (mt-UPR) that can contribute to decreased mitochondrial activity in *etfa*$^{+/-}$ livers (Fig. 7D,E). In a preliminary study, we examined mRNA expression of mt-UPR genes[35] (Supporting Fig. S2) and found a significant increase in *caseinolytic mitochondrial matrix peptidase proteolytic subunit* (*clpp*), *mitochondrial heat shock protein family D member 1* (*hspd1*), and *hspe1* in *etfa*$^{+/-}$ livers; additionally riboflavin supplementation attenuated increased mRNA expression levels of those genes. In aggregate, the data suggest that FAD is a key cofactor to regulate mt-UPR in the liver.

Given the role of ETF as an electron acceptor during fatty acid β-oxidation, reduced ETF function by *etfa* haploinsufficiency results in FAD reduction, which elevates a chance for electron leakage within mitochondria. Leaked electrons generate superoxides, and then superoxides can be converted to H_2O_2 by mitochondrial superoxide dismutase (Sod2; Fig. 5E). Excess H_2O_2 may deplete GSH, which results in accumulation of oxidized toxic molecules, such as MDA in the liver (Fig. 5C). Thus, our data showed that FAD reduction is the key upstream factor underlying *etfa* haploinsufficiency-mediated hepatic injury.

A dramatic increase in *nox1* mRNA expression suggests that Nox1 may play a key role in superoxide

formation by *etfa* haploinsufficiency in addition to superoxides generated by leaked electrons during fatty acid β-oxidation. An important future study will be whether genetic depletion of *nox1* can mitigate oxidative stress and hepatic abnormalities in *etfa*$^{+/-}$ mutants.

Previously, we found that hepatomegaly in the liver of *etfa* homozygous mutant larvae may result from increased mammalian target of rapamycin complex 1 (mTORC1) signaling activity.[16] We found that *etfa* haploinsufficiency was enough to induce mTORC1 signaling in hepatocytes (Supporting Fig. S3). However, increased mTORC1 signaling was observed in some hepatocytes, which was not enough to cause hepatomegaly in *etfa*$^{+/-}$ adult zebrafish unlike *etfa*$^{-/-}$ mutant larvae. Although increased mTORC1 signaling may contribute to cell hypertrophy in some hepatocytes, activation of mTORC1 signaling may be part of a compensatory response to attenuate steatosis in *etfa*$^{+/-}$ liver. Because a previous report showed that liver-specific mTORC1 activation in mice attenuated high-fat diet-induced steatosis in the liver,[36] it is possible that the activation of mTORC1 signaling in *etfa*$^{+/-}$ mutants might be a compensatory response to resolve steatosis by increasing mitochondrial biogenesis (Fig. 7A,B). Previously, we found mitochondrial swelling and cristae injury in *etfa*$^{-/-}$ larvae. Reduced mitochondrial OCR and mitochondrial membrane potential raises the possibility that *etfa* haploinsufficiency may be an important cause of mitochondrial dysfunction and mitochondrial injury. Electron microscopic analysis showed that normal-appearing hepatocytes in *etfa*$^{+/-}$ animals did not develop mitochondrial cristae injury or become swollen as in *etfa*$^{-/-}$ larvae liver. However, we found abnormal cristae structure and endoplasmic reticulum (ER) fragmentation in injured hepatocytes in the *etfa*$^{+/-}$ liver (Supporting Fig. S4). This result suggests that *etfa* haploinsufficiency may cause mitochondrial injury and ER stress, which may lead to hepatic necrosis.

Importantly, newborn screening for ETF deficiency indicates that approximately one in 460 (0.2%) newborns (about 700,000 of the U.S. population) carry a heterozygous deleterious mutation in one of the ETF/ETFDH complex genes. Although mutations in *ETFA* have not been identified in genome-wide association studies (GWASs) in patients with nonalcoholic fatty liver disease[37,38] because a GWAS targets common polymorphisms rather than rare mutations, we speculate that this mutation may predispose this group to fatty liver disease.

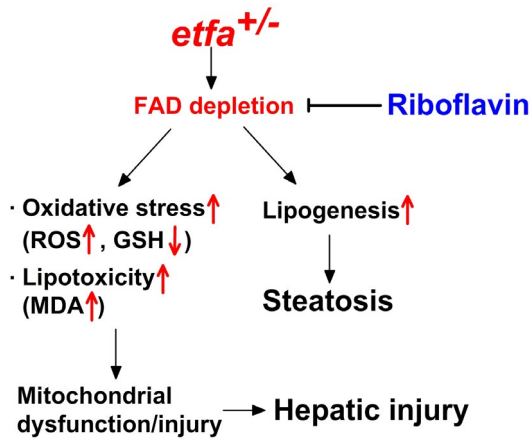

FIG. 8. Diagram demonstrating *etfa* haploinsufficiency-induced hepatic steatosis and injury. *Etfa* haploinsufficiency causes FAD reduction in the liver, which in turn increases lipogenesis/steatosis in the liver. Additionally, increased oxidative stress and lipotoxicity by FAD depletion lead to mitochondrial dysfunction/injury that causes hepatocellular injury.

In summary, we have demonstrated that FAD reduction in *etfa*$^{+/-}$ zebrafish caused hepatic steatosis and injury through increased *de novo* lipogenesis, oxidative stress, and lipotoxicity in the liver (Fig. 8). Riboflavin supplementation essentially reversed the liver abnormalities in *etfa*$^{+/-}$ mutants. As these liver abnormalities (steatosis and hepatic injury) are typical of fatty liver disease, we speculate that *etfa* haploinsufficiency may be a risk factor that can potentiate hepatic steatosis and injury in alcoholic or nonalcoholic steatohepatitis.

Acknowledgment: We thank Danyelle Townsend and Analytic Redox Biochemistry Core Facility for ROS, GSH, and GSSG determination; Yanhui Su for zebrafish husbandry; and John Lemasters, Josh Lipschutz, Deepak Nihalani, Glenn Lobo, and Daria Ilatovskaya for helpful comments.

REFERENCES

1) Lee WS, Sokol RJ. Mitochondrial hepatopathies: advances in genetics and pathogenesis. Hepatology 2007;45:1555-1565.
2) Rinaldo P, Matern D, Bennett MJ. Fatty acid oxidation disorders. Annu Rev Physiol 2002;64:477-502.
3) Frerman FE. Acyl-CoA dehydrogenases, electron transfer flavoprotein and electron transfer flavoprotein dehydrogenase. Biochem Soc Trans 1988;16:416-418.

4) Hauge JG, Crane FL, Beinert H. On the mechanism of dehydrogenation of fatty acyl derivatives of coenzyme A. III. Palmityl coA dehydrogenase. J Biol Chem 1956;219:727-733.
5) Frerman FE, Goodman SI. Defects of electron transfer flavoprotein and electron transfer flavoprotein-ubiquinone oxidoreductase: glutaric acidemia type II. In: Scriver CR, Beaudet AL, Valle D, Sly WS, Childs B, Kinzler, KW, et al. eds. The Metabolic and Molecular Bases of Inherited Disease. 8th ed. New York, NY: McGraw-Hill; 2001:2357-2365.
6) Colevas AD, Edwards JL, Hruban RH, Mitchell GA, Valle D, Hutchins GM. Glutaric acidemia type II. Comparison of pathologic features in two infants. Arch Pathol Lab Med 1988;112:1133-1139.
7) Onkenhout W, Venizelos V, Scholte HR, De Klerk JB, Poorthuis BJ. Intermediates of unsaturated fatty acid oxidation are incorporated in triglycerides but not in phospholipids in tissues from patients with mitochondrial beta-oxidation defects. J Inherit Metab Dis 2001;24:337-344.
8) Lan MY, Fu MH, Liu YF, Huang CC, Chang YY, Liu JS, et al. High frequency of ETFDH c.250G>A mutation in Taiwanese patients with late-onset lipid storage myopathy. Clin Genet 2010;78:565-569.
9) Dusheiko G, Kew MC, Joffe BI, Lewin JR, Path FF, Mantagos S, et al. Recurrent hypoglycemia associated with glutaric aciduria type II in an adult. N Engl J Med 1979;301:1405-1409.
10) Yıldız Y, Talim B, Haliloglu G, Topaloglu H, Akçören Z, Dursun A, et al. Determinants of riboflavin responsiveness in multiple Acyl-CoA dehydrogenase deficiency. Pediatr Neurol 2019;99:69-75.Erratum in: Pediatr Neurol 2020;103:91.
11) Crane FL, Beinert H. On the mechanism of dehydrogenation of fatty acyl derivatives of coenzyme A. II. The electron-transferring flavoprotein. J Biol Chem 1956;218:717-731.
12) Toogood HS, van Thiel A, Basran J, Sutcliffe MJ, Scrutton NS, Leys D. Extensive domain motion and electron transfer in the human electron transferring flavoprotein medium chain Acyl-CoA dehydrogenase complex. J Biol Chem 2004;279:32904-32912.
13) Watmough NJ, Frerman FE. The electron transfer flavoprotein: ubiquinone oxidoreductases. Biochim Biophys Acta 2010;1797: 1910-1916.
14) Barile M, Giancaspero TA, Brizio C, Panebianco C, Indiveri C, Galluccio M, et al. Biosynthesis of flavin cofactors in man: implications in health and disease. Curr Pharm Des 2013;19:2649-2675.
15) Lienhart WD, Gudipati V, Macheroux P. The human flavoproteome. Arch Biochem Biophys 2013;535:150-162.
16) Kim SH, Scott SA, Bennett MJ, Carson RP, Fessel J, Brown HA, et al. Multi-organ abnormalities and mTORC1 activation in zebrafish model of multiple acyl-CoA dehydrogenase deficiency. PLoS Genet 2013;9:e1003563.
17) Park KH, Ye ZW, Zhang J, Kim SH. Palmitic acid-enriched diet induces hepatic steatosis and injury in adult zebrafish. Zebrafish 2019;16:497-504.
18) Zang L, Shimada Y, Nishimura Y, Tanaka T, Nishimura N. A novel, reliable method for repeated blood collection from aquarium fish. Zebrafish 2013;10:425-432.
19) Manevich Y, Hutchens S, Tew KD, Townsend DM. Allelic variants of glutathione S-transferase P1–1 differentially mediate the peroxidase function of peroxiredoxin VI and alter membrane lipid peroxidation. Free Radic Biol Med 2013;54:62-70.
20) Rahn JJ, Stackley KD, Chan SS. Opa1 is required for proper mitochondrial metabolism in early development. PLoS One 2013;8:e59218.
21) Reschly EJ, Bainy A, Mattos J, Hagey LR, Bahary N, Mada SR, et al. Functional evolution of the vitamin D and pregnane X receptors. BMC Evol Biol 2007;7:222.
22) Ribas V, Garcia-Ruiz C, Fernandez-Checa JC. Glutathione and mitochondria. Front Pharmacol 2014;5:151.
23) Imai H, Matsuoka M, Kumagai T, Sakamoto T, Koumura T. Lipid peroxidation-dependent cell death regulated by GPx4 and ferroptosis. Curr Top Microbiol Immunol 2017;403:143-170.
24) Valero T. Mitochondrial biogenesis: pharmacological approaches. Curr Pharm Des 2014;20:5507-5509.
25) Gershoff SN, Andrus SB, Hegsted DM. The effect of the carbohydrate and fat content of the diet upon the riboflavin requirement of the cat. J Nutr 1959;68:75-88.
26) Taniguchi M, Nakamura M. Effects of riboflavin deficiency on the lipids of rat liver. J Nutr Sci Vitaminol (Tokyo) 1976;22:135-146.
27) Tang J, Hegeman MA, Hu J, Xie M, Shi W, Jiang Y, et al. Severe riboflavin deficiency induces alterations in the hepatic proteome of starter Pekin ducks. Br J Nutr 2017;118:641-650.
28) Rosenthal WS, Adham NF, Lopez R, Cooperman JM. Riboflavin deficiency in complicated chronic alcoholism. Am J Clin Nutr 1973;26:858-860.
29) Majumdar SK, Shaw GK, Thomson AD. Vitamin utilization status in chronic alcoholics. Int J Vitam Nutr Res 1981;51:54-58.
30) Pinto J, Huang YP, Rivlin RS. Mechanisms underlying the differential effects of ethanol on the bioavailability of riboflavin and flavin adenine dinucleotide. J Clin Invest 1987;79: 1343-1348.
31) Freneaux E, Sheffield VC, Molin L, Shires A, Rhead WJ. Glutaric acidemia type II. Heterogeneity in beta-oxidation flux, polypeptide synthesis, and complementary DNA mutations in the alpha subunit of electron transfer flavoprotein in eight patients. J Clin Invest 1992;90:1679-1686.
32) Saijo T, Tanaka K. Isoalloxazine ring of FAD is required for the formation of the core in the Hsp60-assisted folding of medium chain acyl-CoA dehydrogenase subunit into the assembly competent conformation in mitochondria. J Biol Chem 1995;270:1899-1907.
33) Sato K, Nishina Y, Shiga K. In vitro refolding and unfolding of subunits of electron-transferring flavoprotein: characterization of the folding intermediates and the effects of FAD and AMP on the folding reaction. J Biochem 1996;120:276-285.
34) Henriques BJ, Rodrigues JV, Olsen RK, Bross P, Gomes CM. Role of flavinylation in a mild variant of multiple acyl-CoA dehydrogenation deficiency: a molecular rationale for the effects of riboflavin supplementation. J Biol Chem 2009;284: 4222-4229.
35) Yi HS, Chang JY, Shong M. The mitochondrial unfolded protein response and mitohormesis: a perspective on metabolic diseases. J Mol Endocrinol 2018;61:R91-R105.
36) Kenerson HL, Yeh MM, Yeung RS. Tuberous sclerosis complex-1 deficiency attenuates diet-induced hepatic lipid accumulation. PLoS One 2011;6:e18075.
37) Sookoian S, Pirola CJ. Genetic predisposition in nonalcoholic fatty liver disease. Clin Mol Hepatol 2017;23:1-12.
38) Romeo S, Kozlitina J, Xing C, Pertsemlidis A, Cox D, Pennacchio LA, et al. Genetic variation in PNPLA3 confers susceptibility to nonalcoholic fatty liver disease. Nat Genet 2008;40:1461-1465.

Supporting Information

Additional Supporting Information may be found at onlinelibrary.wiley.com/doi/10.1002/hep4.1691/suppinfo.